

Dear Author,

Here are the proofs of your article.

- You can submit your corrections **online**, via **e-mail** or by **fax**.
- For **online** submission please insert your corrections in the online correction form. Always indicate the line number to which the correction refers.
- You can also insert your corrections in the proof PDF and **email** the annotated PDF.
- For fax submission, please ensure that your corrections are clearly legible. Use a fine black pen and write the correction in the margin, not too close to the edge of the page.
- Remember to note the **journal title**, **article number**, and **your name** when sending your response via e-mail or fax.
- **Check** the metadata sheet to make sure that the header information, especially author names and the corresponding affiliations are correctly shown.
- **Check** the questions that may have arisen during copy editing and insert your answers/ corrections.
- **Check** that the text is complete and that all figures, tables and their legends are included. Also check the accuracy of special characters, equations, and electronic supplementary material if applicable. If necessary refer to the *Edited manuscript*.
- The publication of inaccurate data such as dosages and units can have serious consequences. Please take particular care that all such details are correct.
- Please **do not** make changes that involve only matters of style. We have generally introduced forms that follow the journal's style. Substantial changes in content, e.g., new results, corrected values, title and authorship are not allowed without the approval of the responsible editor. In such a case, please contact the Editorial Office and return his/her consent together with the proof.
- If we do not receive your corrections **within 48 hours**, we will send you a reminder.
- Your article will be published **Online First** approximately one week after receipt of your corrected proofs. This is the **official first publication** citable with the DOI. **Further changes are, therefore, not possible.**
- The **printed version** will follow in a forthcoming issue.

Please note

After online publication, subscribers (personal/institutional) to this journal will have access to the complete article via the DOI using the URL: [http://dx.doi.org/\[DOI\]](http://dx.doi.org/[DOI]).

If you would like to know when your article has been published online, take advantage of our free alert service. For registration and further information go to: <http://www.springerlink.com>.

Due to the electronic nature of the procedure, the manuscript and the original figures will only be returned to you on special request. When you return your corrections, please inform us if you would like to have these documents returned.

Metadata of the article that will be visualized in OnlineFirst

Please note: Images will appear in color online but will be printed in black and white.

| | | |
|----------------------|--|---|
| ArticleTitle | Self-organizing maps for texture classification | |
| Article Sub-Title | | |
| Article CopyRight | Springer-Verlag London Limited (This will be the copyright line in the final PDF) | |
| Journal Name | Neural Computing and Applications | |
| Corresponding Author | Family Name | Petrov |
| | Particle | |
| | Given Name | Nedyalko |
| | Suffix | |
| | Division | |
| | Organization | School of Computing, University of Portsmouth |
| | Address | PO1 3HE, Portsmouth, England, UK |
| | Email | Nedyalko.Petrov@port.ac.uk |
| Author | Family Name | Georgieva |
| | Particle | |
| | Given Name | Antoniya |
| | Suffix | |
| | Division | |
| | Organization | NDOG, University of Oxford |
| | Address | OX3 9DU, Oxford, England, UK |
| | Email | Antoniya.Georgieva@obs-gyn.ox.ac.uk |
| Author | Family Name | Jordanov |
| | Particle | |
| | Given Name | Ivan |
| | Suffix | |
| | Division | |
| | Organization | School of Computing, University of Portsmouth |
| | Address | PO1 3HE, Portsmouth, England, UK |
| | Email | Ivan.Jordanov@port.ac.uk |
| Schedule | Received | 4 March 2011 |
| | Revised | |
| | Accepted | 26 December 2011 |
| Abstract | A further investigation of our intelligent machine vision system for pattern recognition and texture image classification is discussed in this paper. A data set of 335 texture images is to be classified into several classes, based on their texture similarities, while no a priori human vision expert knowledge about the classes is available. Hence, unsupervised learning and self-organizing maps (SOM) neural networks are used for solving the classification problem. Nevertheless, in some of the experiments, a supervised texture analysis method is also considered for comparison purposes. Four major experiments are conducted: in the first one, classifiers are trained using all the extracted features without any statistical preprocessing; in the second simulation, the available features are normalized before being fed to a classifier; in the third experiment, the trained classifiers use linear transformations of the original features, received after preprocessing with principal component analysis; and in the last one, transforms of the features obtained after applying linear discriminant analysis are used. During the simulation, each test is performed 50 times implementing the proposed algorithm. Results | |

from the employed unsupervised learning, after training, testing, and validation of the SOMs, are analyzed and critically compared with results from other authors.

Keywords (separated by '-') Self-organizing maps - Texture classification - Feature extraction - Statistical analysis - PCA - LDA

Footnote Information

Journal: 521
Article: 797



Author Query Form

**Please ensure you fill out your response to the queries raised below
and return this form along with your corrections**

Dear Author

During the process of typesetting your article, the following queries have arisen. Please check your typeset proof carefully against the queries listed below and mark the necessary changes either directly on the proof/online grid or in the 'Author's response' area provided below

| Query | Details required | Author's response |
|--------------|---|--------------------------|
| 1. | Please confirm the inserted city name is correct and amend if necessary. | |
| 2. | As per the information provided by the publisher, Fig. 8 will be black and white in print; hence, kindly consider rephrasing the caption without referring to colours | |
| 3. | Please provide a definition for the significance of bold values in tables 4, 8. | |
| 4. | Please check and approve the edit made in the article title. | |

2 **Self-organizing maps for texture classification**

3 Nedyalko Petrov · Antoniya Georgieva · Ivan Jordanov

4 Received: 4 March 2011 / Accepted: 26 December 2011
5 © Springer-Verlag London Limited 2011

6 **Abstract** A further investigation of our intelligent
7 machine vision system for pattern recognition and texture
8 image classification is discussed in this paper. A data set of
9 335 texture images is to be classified into several classes,
10 based on their texture similarities, while no a priori human
11 vision expert knowledge about the classes is available.
12 Hence, unsupervised learning and self-organizing maps
13 (SOM) neural networks are used for solving the classifi-
14 cation problem. Nevertheless, in some of the experiments,
15 a supervised texture analysis method is also considered for
16 comparison purposes. Four major experiments are con-
17 ducted: in the first one, classifiers are trained using all the
18 extracted features without any statistical preprocessing; in
19 the second simulation, the available features are normal-
20 ized before being fed to a classifier; in the third experiment,
21 the trained classifiers use linear transformations of the
22 original features, received after preprocessing with princi-
23 pal component analysis; and in the last one, transforms of
24 the features obtained after applying linear discriminant
25 analysis are used. During the simulation, each test is per-
26 formed 50 times implementing the proposed algorithm.
27 Results from the employed unsupervised learning, after
28 training, testing, and validation of the SOMs, are analyzed
29 and critically compared with results from other authors.
30

Keywords Self-organizing maps · Texture classification · 31
Feature extraction · Statistical analysis · PCA · LDA 32

1 Introduction 33

Analysis, recognition, and classification of texture patterns 34
and images are topics with current surge of research 35
interest in the field of digital image processing and pattern 36
recognition, with wide areas of applications [1–5]. A 37
number of different methods, algorithms, and paradigms 38
have been or are being developed nowadays [6–9]. 39

The investigated image classification and recognition 40
systems may vary in their approach but most of them include 41
data acquisition, data preprocessing, feature extraction, 42
feature analysis, classification, and testing and evaluation 43
stages [8–11]. The preprocessing of the raw data is difficult 44
but important part of the whole process, whose aims are to 45
extract useful and appropriate characteristics and features 46
that are to be used in the later stages [8]. Often, the raw data 47
are too large or complex to be used directly as input to a 48
classifier, leading to the “curse of dimensionality” and other 49
problems related to the generalization abilities of the trained 50
systems, especially when insufficient training samples are 51
available. Even if this is not the case, reducing the number of 52
variables representing the data can speed up and facilitate the 53
learning process at later stages [11]. That is why principal 54
component analysis (PCA), for example, is a widely accep- 55
ted technique in such cases [1, 2, 12]. 56

In [12], we investigated a classification of texture images 57
problem, using supervised neural network learning, for 58
which a priori knowledge about the image classes was used. 59

The aim of this research is to extend this previous work, 60
considering the same classification problem, but assuming 61
there is no expert knowledge available for the texture 62

A1 N. Petrov (✉) · I. Jordanov
A2 School of Computing, University of Portsmouth,
A3 Portsmouth PO1 3HE, England, UK
A4 e-mail: Nedyalko.Petrov@port.ac.uk

A5 I. Jordanov
A6 e-mail: Ivan.Jordanov@port.ac.uk

A7 A. Georgieva
A8 NDOG, University of Oxford, Oxford OX3 9DU, England, UK
A9 e-mail: Antoniya.Georgieva@obs-gyn.ox.ac.uk

63 classes of the data set samples. This implies that no
64 supervised learning can be used, and the knowledge about
65 the texture patterns and their similarity and uniformity has
66 to be extracted from the data set itself. Unsupervised
67 classification of texture patterns and images is widely used
68 approach with applications in a broad range of areas, for
69 example: for determining water quality based on some
70 chemical and physicochemical features [1], for classifica-
71 tion of SAR images [2], for texture-based classification of
72 atherosclerotic carotid plaque images for determining risk
73 of stroke for individuals [13], for classifying volcanic ash
74 using surface texture features [3], for automatically clas-
75 sifying texture structure of different fabric types using
76 SOM [14], for classification of textures in scene images
77 using biology inspired features [6], for classification of
78 aerial images using SOMs [15].

79 In this investigation, a data set of 335 texture images,
80 acquired via an intelligent visual recognition system, as
81 reported in [12], is used. Each data sample of the set rep-
82 resents a grayscale image of an industrial cork tile that was
83 classified in the previous paper into one of seven classes—
84 *Beach*, *Corkstone*, *Desert*, *Lisbon*, *Pebble*, *Precision* and
85 *Speckled*. The distribution of the texture classes is non-
86 uniform and is shown in Fig. 1.

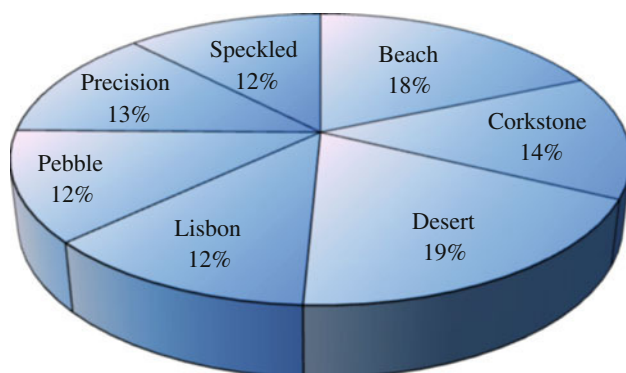
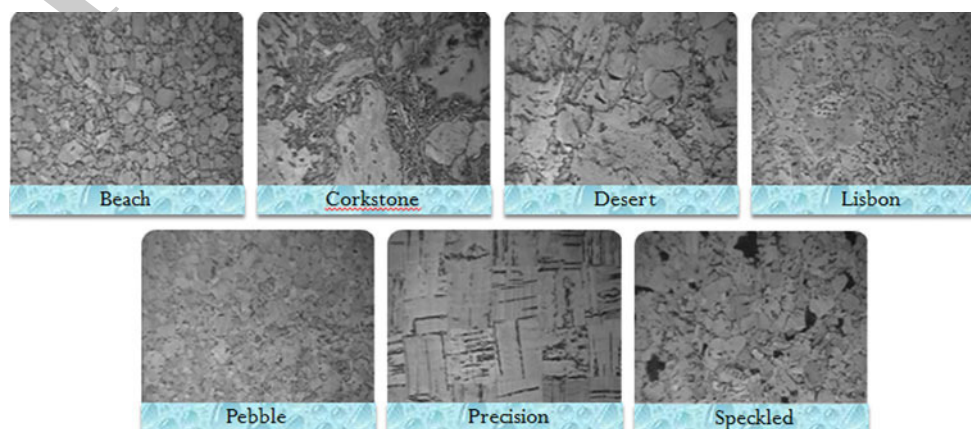


Fig. 1 Distribution of the texture classes

Fig. 2 Samples of the acquired texture data—images of seven different types of wall cork tiles: *Beach*, *Corkstone*, *Desert*, *Lisbon*, *Pebble*, *Precision* and *Speckled*



87 The simulation of the investigated system is divided in
88 five main stages: data acquisition, feature extraction, fea-
89 ture analysis, classifier training, and classifier testing and
90 evaluation.

91 The rest of the paper is organized as follows: Sect. 2 pre-
92 sents information about the data acquisition, feature extrac-
93 tion, and feature analysis and reduction stages, while Sect. 3
94 covers the classification stage. The results from the conducted
95 tests are given and discussed in Sect. 4. Finally, Sect. 5 con-
96 cludes the paper and gives some ideas for future work.

97 2 Data acquisition and feature extraction

98 The texture image data set used in this paper is acquired via
99 an intelligent visual recognition system described in more
100 detail in [12]. The system consists of a charge-coupled
101 device camera, lightning devices, and scaffolding. Since
102 the texture of the samples is of prime interest, the images
103 are converted to a grayscale format.

104 As mentioned above, a total of 335 grayscale images of
105 size 230×340 pixels of cork tile samples of 7 predefined
106 by experts types were collected (see Fig. 2).

107 The feature extraction phase in our investigation aims to
108 identify characteristics and properties that make the classes
109 of samples distinct from each other [16]. At this stage of
110 the process, features that represent some valuable infor-
111 mation about the texture of the images are obtained. This is
112 preceded by image normalization.

113 2.1 Initial feature extraction

114 In order to reduce the illumination effects on the analyzed
115 images (e.g., due to a glare), a normalization technique is
116 applied. In this process, a small window (15×15 pixels) is
117 moved within each image and the local average is subtracted
118 from the pixels' values, in order to get images with average
119 intensity of each neighborhood about a zero [9]. Afterward,
120 34 features are extracted using classical approaches.

121 2.1.1 Co-occurrence matrices

122 Co-occurrence matrices, introduced by Haralick in [17], is
 123 a commonly applied statistical approach for texture fea-
 124 tures extraction that takes into account relative dis-
 125 tances and orientation of pixels with co-occurring values
 126 [9, 15, 18].

127 The MATLAB's Image Processing Toolbox is used for
 128 the computation of the co-occurrence matrices of the nor-
 129 malized images. As usually proposed by other authors [19],
 130 four relative orientations are used—horizontal (0°), right
 131 diagonal (45°), vertical (90°), and left diagonal (135°). In
 132 this way, the *energy*, *homogeneity*, *correlation*, and *con-*
 133 *trast* characteristics in each direction are computed, getting
 134 as a result the rotation invariant features [9, 11].

135 Also, two spatial relationships are considered—the
 136 direct neighbors and the pixels with difference of five. As a
 137 result, a total of eight co-occurrence matrices are
 138 obtained—four for the direct neighbors and another four
 139 for the pixels with difference of five.

140 2.1.2 Laws' masks

141 The Laws' masks are used as a filter technique that is
 142 applied to identify points of high energy in an image [20].
 143 Masks are derived from one-dimensional (1-D) vectors of
 144 five pixels length, proposed by Laws, to pick up the average
 145 gray level, edges, ripples, spots, and waves [12, 13]:

146 L_5 (Level) = [1 4 6 4 1] → Level detection;
 147 E_5 (Edge) = [-1 -2 0 2 1] → Edge detection;
 148 S_5 (Spot) = [-1 0 2 0 -1] → Spot detection;
 149 R_5 (Ripple) = [1 -4 6 -4 1] → Ripple detection;
 150 W_5 (Wave) = [-1 2 0 -2 1] → Wave detection.

151 The vectors are multiplied each other (the second vector
 152 is transposed) and this way 25 different 5×5 masks are
 153 produced. The masks are then applied to the normalized set
 154 of samples and the obtained filtered images are converted
 155 to texture energy maps. The aim of this process (also called
 156 smoothing) is to deduce the local magnitudes of the
 157 quantities of interest (edges, spots, etc.). A smoothing
 158 window of size 15×15 [9] is applied to each filtered
 159 image F_k for the k -th mask and new energy images are
 160 obtained, where each pixel in the image is given by (1):

$$E_k(r, c) = \sum_{j=c-7}^{c+7} \sum_{i=r-7}^{r+7} |F_k(i, j)|, \quad (k = 1, \dots, 25), \quad (1)$$

162 where (r, c) denotes the rows and columns indices. After
 163 obtaining 25 energy maps for each image, a power metric,
 164 representing the sum of the squared absolute values for
 165 each pixel in the map is used [9], to finally obtain 25 dif-
 166 ferent values for each texture sample.

2.1.3 Entropy

Entropy is a statistical measure of randomness that can be
 used to characterize the texture of an image [9, 14]. It takes
 low values for smooth images and vice versa.

The entropy for each image sample is calculated using a
 MATLAB's build-in function, according to (2):

$$E = - \sum_{i=1}^G d(i) \cdot \log_2 d(i), \quad (2)$$

where G is the number of gray levels in the image's his-
 togram, ranging between 0 and 255 for a typical 8-bit
 image, and $d(i)$ is the normalized occurrence frequency of
 each gray level.

2.2 Statistical analysis and feature reduction

Before applying any statistical analysis, a random subset of
 25% of the available data is excluded for the purposes of
 further testing. This subset will be referred to as the testing
 set from now on and the remaining 75% of the available
 data will be the training set.

During the feature extraction stage, a total of 34 features
 are obtained for each texture image (8 by the co-occurrence
 method, 25 by Law's masks and 1 entropy feature). The
 distribution of the seven classes of the training set, repre-
 sented by two randomly selected from the 34 features is
 shown in Fig. 3. Figure 3b presents the classes' distribu-
 tion according to the 2nd and the 5th features of the ori-
 ginal data set and Fig. 3a shows the classes' means with
 95% confidence interval. As it can be seen from Fig. 3, the
 considerable overlap between the classes makes the clas-
 sification process more challenging.

In order to reduce the dimensionality of the classifica-
 tion problem (i.e., the number of inputs to the classifier), to
 reduce the redundant information (i.e., the information
 contained in some highly correlated features), and to
 improve the class separability, two statistical analysis
 techniques [10] are used in some of the experiments. They
 are described in more details in the next two subsections.

2.2.1 Principal component analysis

PCA is an eigenvalue-based multivariate technique that
 transforms a number of possibly correlated features into a
 number of uncorrelated features, called principal compo-
 nents (PC) [2, 9]. The number of the derived PCs is less
 than or equal to the number of the original features. It is an
 unsupervised technique and as such does not use any
 labeled information on the data.

The first PC accounts for as much of the variability
 (information) in the data, as possible, and each succeeding

Fig. 3 Texture types distribution, according to two randomly selected features from the training set: **a** classes' means with 95% confidence intervals; **b** scatter plot of the samples

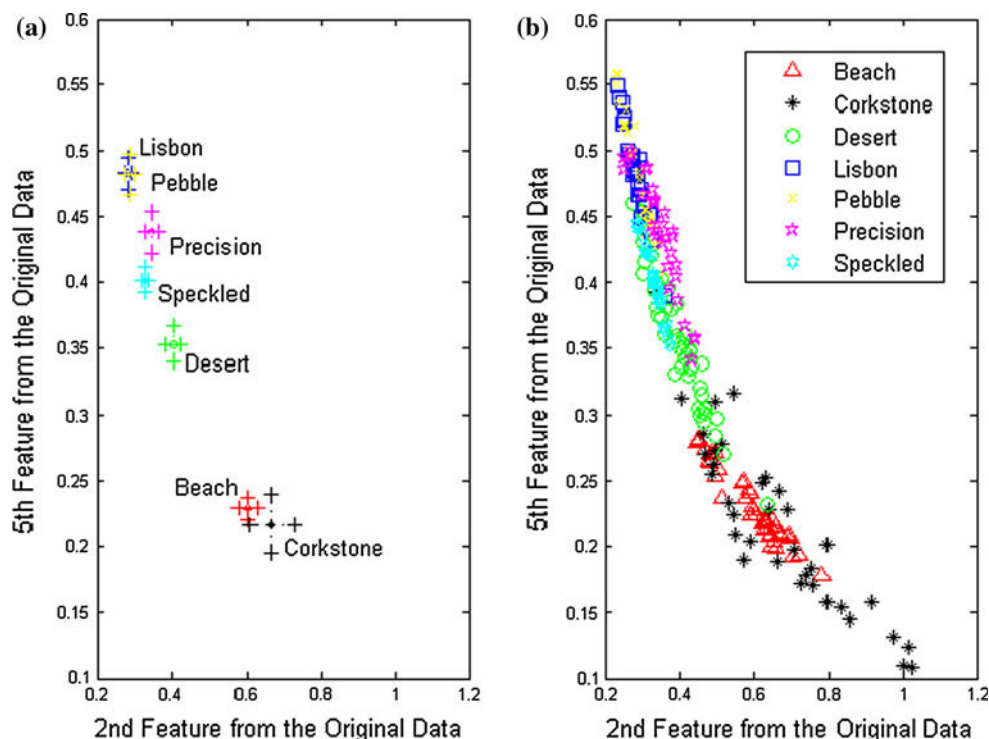
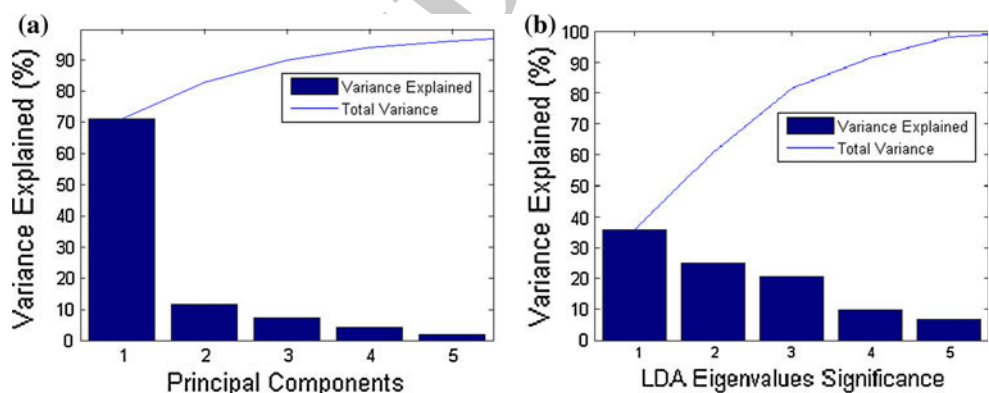


Fig. 4 Percentage of the information from the training set contained: **a** in the first five PCs for the PCA experiment; **b** in the first five eigenvalues for the LDA experiment



212 PC accounts for as much of the remaining variability as
 213 possible. Depending on the areas of application, PCA is
 214 also referred to as Hotelling transform, Karhunen–Loeve
 215 transform, or proper orthogonal decomposition [9].

216 The PCA implementation of the MATLAB's Statistics
 217 Toolbox is used for processing the extracted features of the
 218 training set. As a result, a new data set in which the first 5
 219 features contain about 97% of the total variation (infor-
 220 mation) is obtained (Fig. 4a). The PCA transformation
 221 matrix is saved for further use in the evaluation stage.

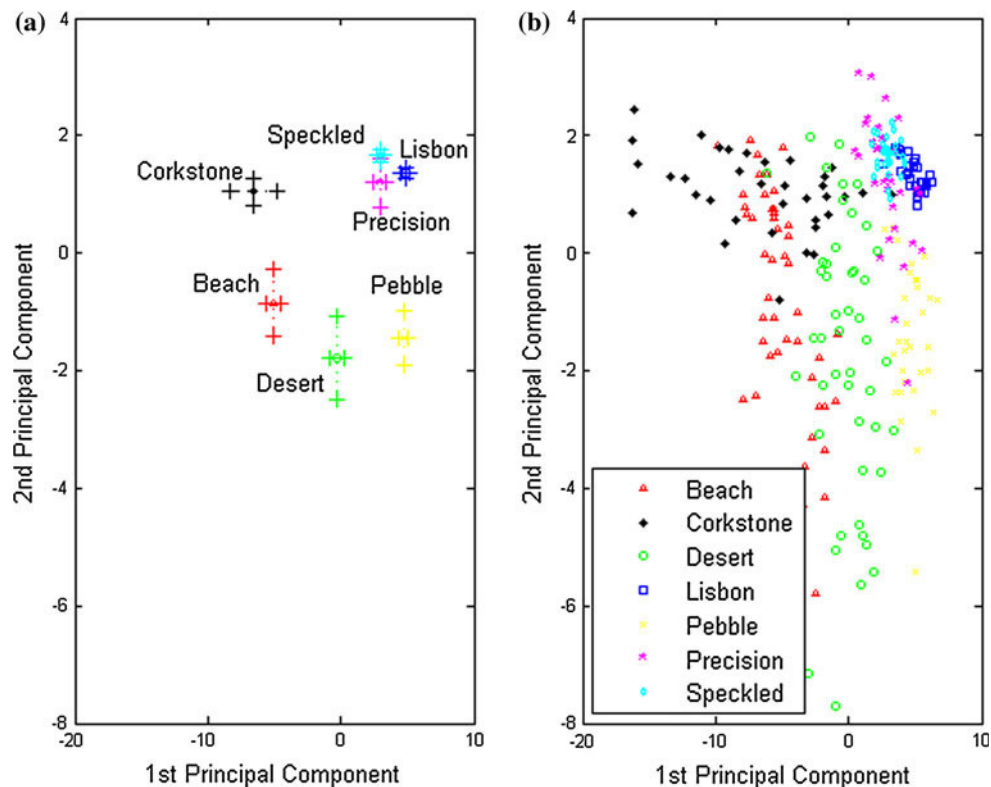
222 Figure 5 shows the distribution of the seven texture
 223 classes, represented by the first and second PCs. It can be
 224 seen that four out of the seven classes (*Beach*, *Corkstone*,
 225 *Desert*, and *Pebble*) are easily separable from the others.
 226 However, the rest of the classes are too close to each other

and partially overlap. This is because the PCA considers all
 227 the data samples independently, without taking into
 228 account which class they belong to. The overlapping in
 229 some of the classes however is expected to harden the
 230 classifiers' performance later on.
 231

2.2.2 Linear discriminant analysis

232
 233 Linear discriminant analysis (LDA) is an eigenvalues-
 234 based transformation technique that aims to find a linear
 235 combination of features that characterize or separate two or
 236 more classes [9, 21]. LDA is not used in this work as a
 237 classification technique, but as a data preprocessing trans-
 238 form, before applying the classification technique, as rec-
 239 ommended in [10]. The number of the newly generated

Fig. 5 Texture types distribution, according to the first two PCs: **a** classes' means with 95% confidence intervals; **b** scatter plot of the samples



240 features is always one less than the number of the classes.
 241 An LDA implementation in MATLAB, following the
 242 algorithm presented in [21], is employed for this research.

243 LDA is applied to the features extracted for each texture
 244 sample of the training set. As a result, the dimensionality of
 245 the feature space is reduced from 34 to 6 without loss of
 246 information about the class separability [11] and the LDA
 247 transformation matrix is saved for further use in the eval-
 248 uation stage.

249 Figure 4b shows the percentage contribution of each
 250 eigenvalue to the sum of the six eigenvalues. It can be seen
 251 that about 98.5% of the eigenvalues sum is contributed by
 252 the first five eigenvalues.

253 The classes' means with 95% confidence intervals and
 254 the scatter plot of the processed with LDA data are shown
 255 in Fig. 6. It can be seen that the classes' separability is
 256 considerably improved.

257 3 Classification

258 For the classification of the texture samples data, self-
 259 organizing maps (SOM) are employed. As it is known, a
 260 SOM is an artificial neural network (NN) that is trained
 261 using unsupervised learning to produce a low-dimensional
 262 (typically two-dimensional), discretized representation of
 263 the input space of the training samples, called map. A
 264 specific characteristic of SOMs (compared to other NNs) is

265 that they use a neighborhood function to preserve the
 266 topological properties of the input space [22]. Like most
 267 neural networks, SOMs operate in two modes: training and
 268 testing. The MATLAB's implementation of SOM is
 269 employed for this research and the following algorithm is
 270 used for the classification:

- 271 1. Design of SOM's architecture (map topology, number
 272 of neurons, training parameters, etc.);
- 273 2. Training of the SOM with data subset, representing the
 274 extracted texture features (75% of the available data set);
- 275 3. As a result of step b), a 2D map is obtained, in which
 276 each node and its closest neighbors represent similar
 277 data samples (Fig. 7);
- 278 4. Based on the available expert knowledge for the
 279 training samples, the count of the samples belonging to
 280 a certain class is determined for each node of the map;
- 281 5. Each node is then labeled to represent just one class—
 282 the class with predominant number of associated
 283 samples. In case equal number of samples of different
 284 classes is mapped to a certain node, the node is labeled
 285 to the predominant class in its neighborhood (Fig. 7).
 286 A node gets no label if there are no data samples
 287 mapped to it (the red node in Fig. 7b);
- 288 6. The classifier's testing is performed with the remaining
 289 25% of the available data;
- 290 7. Each testing sample label is compared to the label of
 291 the node that it is mapped to. A sample is counted as
 292 unclassified if it is mapped to an unlabeled node;

Fig. 6 Texture types distribution, according to the first two eigenvalues: **a** classes' means with 95% confidence intervals; **b** scatter plot of the samples

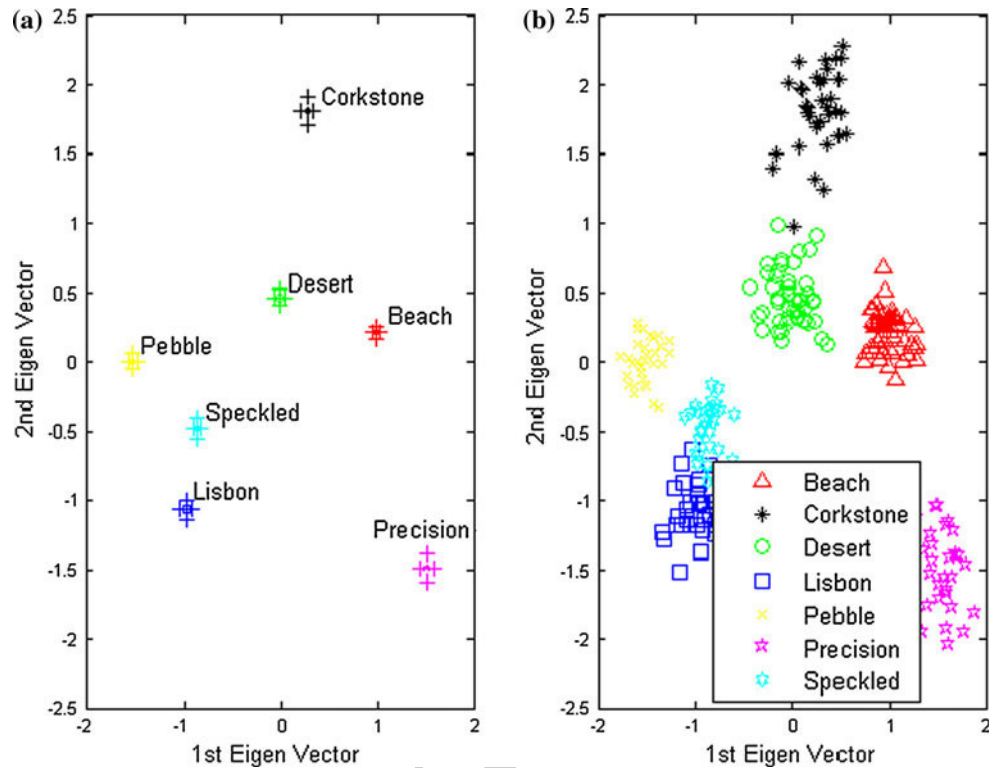
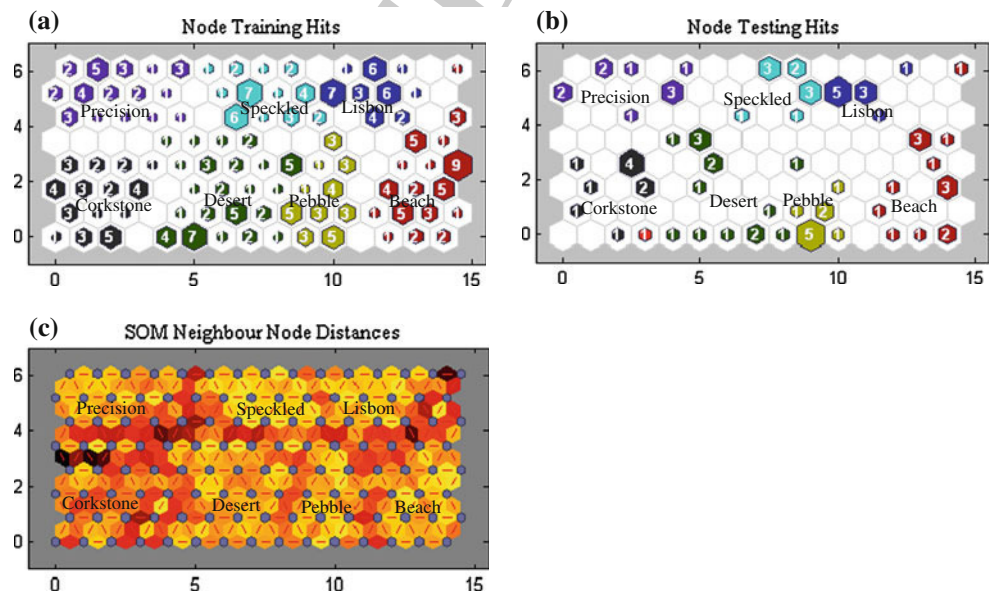


Fig. 7 Sample SOM classifier map. Image **a** presents the node hits for the samples from the training set and **b** from the testing set. The number in each node represents its hits. The nodes are colored according to the classes they are labeled to. Image **c** shows the relative distance between the map nodes. Darker color corresponds to larger distances



293 8. The classification accuracy rate is calculated using
294 Eq. 3:

$$a = \frac{n_c}{n_c + n_w + n_u} \cdot 100[\%], \quad (3)$$

296 where a is the accuracy of the classifier, n_c is the
297 number of correctly classified samples, n_w is the num-
298 ber of wrongly classified samples and n_u is the number
299 of unclassified samples.

4 Simulation and results

MATLAB 2010B and its Neural Network, Image Pro-
cessing and Statistics Toolboxes are used for the compu-
tations and simulations presented in this paper.

Four major experiments are conducted: in the first one,
the classifiers are trained using all the extracted features
without any statistical preprocessing; in the second, the
extracted features are normalized before being fed to a

308 classifier; in the third experiment, the trained classifiers use
309 features obtained after preprocessing with PCA; and in the
310 last one, features obtained after applying LDA are used.

311 During the simulation, each test is performed 50 times
312 using the algorithm given in Sect. 3. The minimum, max-
313 imum, and mean percentages of successfully classified
314 texture images from the testing set are recorded, and the
315 mean standard deviation over the 50 runs is also calculated.

316 4.1 Classification without statistical preprocessing

317 In this experiment, SOMs are trained using all the 34
318 extracted features. No statistical preprocessing is per-
319 formed, and random 75% (251 texture images) of the
320 available data samples are used for training and the
321 remaining 25% (84 texture images) for testing.

322 Tables 1 and 3 show results from simulations with
323 varying number of training epochs and varying number of
324 neurons for different SOM's topologies. The sample con-
325 fusion matrix given in Table 4 shows excellent perfor-
326 mance of the classifier for two of the classes (Lisbon and
327 Speckled) and inferior results for the rest.

328 4.2 Classification with features normalization

329 In this experiment, all 34 features are used for the SOM's
330 learning and the training set is normalized, so that the
331 features have zero mean and unity standard deviation.
332 Tables 2 and 3 show results from simulations with varying
333 number of training epochs and varying number of neurons
334 for different SOM's topologies. Table 4 gives a sample
335 confusion matrix of the classifier's performance for one

Table 1 Variation of the classifier's accuracy (in %) for different number of training epochs and no statistical preprocessing

| Epochs | 50 | 100 | 250 | 500 | 1,000 | 2,500 | 5,000 | 7,500 |
|--------|------|------|------|------|-------|-------|-------|-------|
| Min | 48.2 | 58.0 | 70.3 | 70.4 | 75.3 | 75.3 | 74.1 | 75.3 |
| Max | 63.0 | 75.3 | 81.5 | 80.3 | 81.5 | 81.5 | 82.7 | 82.7 |
| Mean | 55.1 | 66.7 | 77.0 | 77.0 | 78.4 | 78.3 | 78.0 | 78.1 |
| Std | 3.6 | 3.9 | 2.6 | 1.9 | 1.4 | 1.6 | 1.9 | 1.8 |

SOMs with 120 neurons (15×8 map topology) are trained

Table 2 Variation of the classifier's accuracy (in %) for different number of training epochs for SOM with 120 neurons (15×8 map topology) after normalization

| Epochs | 50 | 100 | 250 | 500 | 1,000 | 2,500 | 5,000 | 7,500 |
|--------|------|------|------|------|-------|-------|-------|-------|
| Min | 71.6 | 79.0 | 84.0 | 84.0 | 85.2 | 85.2 | 87.7 | 87.7 |
| Max | 86.4 | 90.1 | 93.8 | 93.8 | 93.8 | 93.8 | 95.1 | 93.8 |
| Mean | 77.8 | 84.9 | 88.7 | 89.8 | 89.9 | 89.8 | 90.8 | 90.9 |
| Std | 3.6 | 3.1 | 2.4 | 2.0 | 2.1 | 1.8 | 1.8 | 1.6 |

run. It can be seen that the classifier's performance is
improved, and it is now able to better distinguish most of
the classes. However, it still experiences some difficulties
with the *Beach* and the *Corkstone* samples.

4.3 Classification with PCA

In this case, statistically preprocessed with PCA data is
used for the training of SOMs. Again, random 75% (251
texture images) of the available data samples are used for
training and the remaining 25% (84 texture images) for
testing.

Similarly to the previous case, the number of training
epochs, the number of neurons in the SOM, the SOM's
topology, and the number of principal components (PC)
used for the training are varied. Each sub-experiment is
performed 50 times, and the minimal, maximal, and the
mean accuracy (%) for these runs are recorded. The results
are presented in Tables 5, 7, and Fig. 8a. The sample
confusion matrix given in Table 8 shows that this classifier
experience slight difficulties recognizing some of the
Corkstone samples, but performs very well on the rest of
the classes.

4.4 Classification with LDA

In the last experiment, SOMs are trained using data sta-
tistically preprocessed with LDA, while the same training/
testing data ratio (75% training, 25% testing) is kept intact.

The parameters for this experiment are varied through
the number of eigenvalues used, the number of training
epochs, the number of neurons, and the SOM's topology.
Each simulation is performed 50 times, and the minimal,
maximal, and the mean accuracy (in %) for these runs are
given in Fig. 8b, Tables 6, and 7. Table 8 presents a
sample confusion matrix of the classifier's performance for
one run. It can be seen that this classifier is able to dis-
tinguish all the classes, and the classification error is
mainly contributed by the unclassified samples (mapped to
an unlabeled node).

4.5 Analysis of the results

Figure 8a illustrates that no significant improvement of the
accuracy is obtained when more than 5 principal compo-
nents are used (PCA case), and for the LDA case (Fig. 8b),
the first 3 eigenvalues bring the most significant improve-
ment. This could also be concluded from the graphics
given in Fig. 4.

Regarding the SOM's topology, no clear correlation
between the accuracy and the number of used neurons was
observed (Tables 3 and 7), but more experiments need to
be done in order to investigate this in more detail.

Table 3 Variation of the classifier's accuracy (in %) for different number of neurons and different SOM topology (trained for 500 epochs): with no statistical preprocessing on the left side of the cells and after normalization on the right

| Neurons | 60 | | | 120 | | |
|---------|-----------|-----------|-----------|-----------|-----------|-----------|
| | 3 × 20 | 5 × 12 | 6 × 10 | 6 × 20 | 10 × 12 | 12 × 10 |
| Min | 70.4/82.7 | 69.1/84.0 | 69.1/85.2 | 67.9/84.0 | 70.4/84.0 | 70.4/85.2 |
| Max | 82.7/92.6 | 79.0/92.6 | 80.3/92.6 | 81.5/93.8 | 81.5/92.6 | 81.5/92.6 |
| Mean | 77.9/88.0 | 75.2/88.1 | 75.1/87.9 | 75.5/88.1 | 75.9/89.0 | 76.6/89.1 |
| Std | 2.5/2.0 | 2.4/2.1 | 2.3/2.0 | 2.9/2.0 | 2.0/1.9 | 2.5/1.6 |

Table 4 Sample confusion matrix for SOM classifier with 120 neurons (15 × 8 map topology) and 500 training epochs: with no statistical preprocessing on the left side of the cells and after normalization on the right

| Actual | Predicted | | | | | | | |
|-----------|--------------|------------|--------------|--------------|-------------|-------------|------------|--------------|
| | Beach | Corkstone | Desert | Lisbon | Pebble | Precision | Speckled | Unclassified |
| Beach | 14/13 | 1/1 | 0/0 | 0/0 | 0/0 | 0/0 | 0/0 | 0/1 |
| Corkstone | 1/0 | 8/7 | 0/1 | 0/0 | 1/2 | 0/0 | 0/0 | 1/1 |
| Desert | 2/0 | 0/0 | 10/15 | 0/0 | 1/0 | 1/0 | 1/0 | 0/0 |
| Lisbon | 0/0 | 0/0 | 0/0 | 11/11 | 0/0 | 0/0 | 0/0 | 0/0 |
| Pebble | 0/0 | 1/0 | 0/1 | 2/0 | 8/10 | 0/0 | 0/0 | 0/0 |
| Precision | 1/0 | 0/0 | 1/0 | 1/1 | 2/0 | 5/10 | 1/0 | 0/0 |
| Speckled | 0/0 | 0/0 | 0/0 | 1/0 | 0/1 | 0/0 | 9/9 | 0/0 |

Table 5 Variation of the accuracy (in %) of the classifier for different number of training epochs for SOM with 120 neurons, 15 × 8 map topology, and PCA preprocessing with 5 PCs

| Epochs | 50 | 100 | 250 | 500 | 1,000 | 2,500 | 5,000 | 7,500 |
|--------|------|------|------|------|-------|-------|-------|-------|
| Min | 70.4 | 74.1 | 85.2 | 85.2 | 85.2 | 84.0 | 85.2 | 86.4 |
| Max | 85.2 | 88.9 | 92.6 | 91.4 | 93.8 | 92.6 | 92.6 | 92.6 |
| Mean | 75.6 | 80.9 | 89.1 | 88.8 | 89.2 | 88.9 | 89.5 | 89.3 |
| Std | 2.8 | 3.3 | 2.1 | 1.6 | 2.0 | 1.8 | 1.5 | 1.5 |

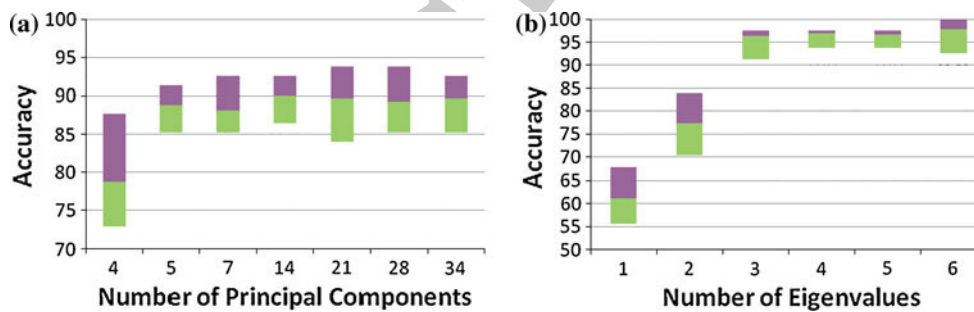


Fig. 8 Variation of the accuracy (in %) of the classifier (SOM with 120 neurons, 15 × 8 map topology, 500 epochs). The border between the subbars shows the mean accuracy rate for the 50 runs. The green

and the purple sections show the min and max rate, respectively, for: a different number of PCs used for the training (after PCA); b different number of eigenvalues used for training (after LDA)

Table 6 Variation of the accuracy (in %) of the classifier for different number of training epochs for SOM with 120 neurons, 15 × 8 map topology, and LDA with 6 eigenvalues

| Epochs | 50 | 100 | 250 | 500 | 1,000 | 2,500 | 5,000 | 7,500 |
|--------|------|------|-------|-------|-------|-------|-------|-------|
| Min | 85.2 | 86.4 | 92.6 | 92.6 | 95.1 | 96.3 | 95.1 | 95.1 |
| Max | 96.3 | 98.8 | 100.0 | 100.0 | 100.0 | 100.0 | 100.0 | 100.0 |
| Mean | 92.6 | 93.9 | 97.7 | 97.9 | 98.5 | 98.2 | 98.1 | 98.2 |
| Std | 2.9 | 3.0 | 1.5 | 1.3 | 1.2 | 1.1 | 1.1 | 1.3 |

Figure 9 summarises and illustrates the obtained results for the four cases, presented in the previous section. It can be seen from the figure that, as expected, the worst accuracy is attained for the case with no statistical preprocessing. Although the accuracy of the normalized data looks better than the obtained one for the PCA case, it has to be noted that only five principal components are considered during the training, whereas in the normalized case, all 34 extracted features are taken into account. The use of only

Table 7 Variation of the classifier's accuracy (in %) for different number of neurons, different SOM topology, 500 epochs after: PCA with 5 PCs on the left side of the cells and LDA with 6 eigenvalues on the right

| Neurons | 60 | | | 120 | | |
|---------|------------|------------|------------|------------|------------|------------|
| | 3 × 20 | 5 × 12 | 6 × 10 | 6 × 20 | 10 × 12 | 12 × 10 |
| Min | 81.5/96.3 | 81.5/96.3 | 82.7/96.3 | 81.5/95.1 | 82.7/93.8 | 84.0/93.8 |
| Max | 91.4/100.0 | 92.6/100.0 | 91.4/100.0 | 93.8/100.0 | 92.6/100.0 | 91.4/100.0 |
| Mean | 86.7/98.7 | 87.8/99.2 | 87.4/99.1 | 87.1/98.6 | 88.7/97.9 | 88.4/97.6 |
| Std | 2.1/1.1 | 2.2/0.9 | 1.8/1.0 | 2.2/1.4 | 2.0/1.2 | 1.7/1.4 |

Table 8 Sample confusion matrix for SOM classifier with 120 neurons (15 × 8 map topology) and 500 training epochs: with PCA on the left side of the cells and with LDA on the right

| Actual | Predicted | | | | | | | |
|-----------|--------------|-------------|--------------|--------------|--------------|--------------|------------|--------------|
| | Beach | Corkstone | Desert | Lisbon | Pebble | Precision | Speckled | Unclassified |
| Beach | 14/15 | 0/0 | 1/0 | 0/0 | 0/0 | 0/0 | 0/0 | 0/0 |
| Corkstone | 0/0 | 7/10 | 1/0 | 0/0 | 2/0 | 0/0 | 0/0 | 1/1 |
| Desert | 1/0 | 0/0 | 14/14 | 0/0 | 0/0 | 0/0 | 0/0 | 0/1 |
| Lisbon | 0/0 | 0/0 | 0/0 | 11/11 | 0/0 | 0/0 | 0/0 | 0/0 |
| Pebble | 0/0 | 0/0 | 0/0 | 0/0 | 11/11 | 0/0 | 0/0 | 0/0 |
| Precision | 0/0 | 0/0 | 0/0 | 1/0 | 0/0 | 10/11 | 0/0 | 0/0 |
| Speckled | 0/0 | 0/0 | 0/0 | 1/0 | 0/1 | 0/0 | 9/9 | 0/0 |

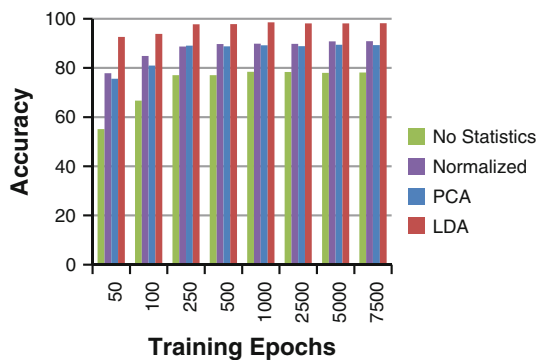


Fig. 9 Bar graph showing the accuracy for the four case studies with increasing the number of training epochs

392 five PCs in the PCA case led to significant reduction in the
 393 computational time, compared to the first two experiments.

394 Analyzing the sample confusion matrices for the four
 395 experiments (Tables 4 and 8), it can be said that the
 396 accuracy is improved (as expected) after applying LDA
 397 and PCA on the data sets, and this is especially valid for the
 398 *Desert* and *Precision* classes, while at the same time, the
 399 SOM kept excellent recognition rate for the *Lisbon* and
 400 *Speckled* classes.

401 Overall, the achieved accuracy for the LDA case is
 402 superior for all runs, outperforming the others by 9% on
 403 average. The best results for the LDA are due to the nature
 404 of this approach, which uses the samples' labels during the
 405 feature analysis. On the contrary, the PCA does not con-
 406 sider the classes when applying orthogonal linear transfor-
 407 mation to convert the investigated features to principal
 408 components. It can also be observed that the increase in the

number of epochs for the runs does not lead to substantial
 increase in the accuracy, and above 250 epochs, an accu-
 racy plateau is normally reached (Tables 1, 2, 5, and 6).

The results for the PCA case, presented in Tables 5 and
 7, are in good agreement with those given in [2], where the
 authors reported between 81 and 98% accuracy rate for a
 PCA-based unsupervised classification of SAR images.
 They are also very close to the [83, 95.5%] achieved in [15]
 and fall within the intervals with slightly larger accuracy
 variance, reported in [5, 6], where the results are within the
 [77, 100%] and [67, 92%] domains, respectively.

5 Conclusion

The investigated texture image recognition of cork tiles is
 considered as unsupervised classification problem, and
 SOMs are employed for its solution. The proposed
 approach includes statistical feature preprocessing tech-
 niques (for the purposes of dimensionality reduction and
 defining optimal number of the features used for the clas-
 sification) and employing SOM as a classifier for unsu-
 pervised classification (NN architecture and topology
 design, investigating the complexity of the unsupervised
 learning and the performance of the SOM). For the purpose
 of comparison, the experiments and simulations of the
 system are also conducted using the raw data set without
 any statistical preprocessing. As expected, better results are
 obtained for the cases when statistical techniques such as
 PCA and LDA are used (on average about 92% accuracy
 rate). When LDA is applied, the trained SOMs achieve

Author Proof

437 very high accuracy rate—above 98%. This can be expected, as LDA is in fact supervised labeling technique, which
438 makes the classification tasks for the subsequently used
439 SOM much easier.

441 The comparison of the sample confusion matrices for
442 the four experiments (Tables 4 and 8) shows that the SOM
443 classifiers generally confirm the experts' knowledge about
444 the seven types of texture. However, the visual closeness of
445 some of the misclassified samples to samples from other
446 classes could assist experts to refine the classes' boundaries
447 or to introduce new classes.

448 Although a straightforward comparison of the methods'
449 performance, based only on the accuracy, can be misleading
450 due to the different complexity of the investigated
451 problems (network's topology parameters, training convergence
452 parameters, differences in the preprocessing techniques,
453 and variations in the number of the investigated features
454 and classes, size and quality of the datasets, etc.), it
455 still can give some indication about the method quality.
456 Nevertheless, as compared with results from other authors
457 in the above paragraph, it can be concluded that while our
458 results of 88% mean accuracy for the PCA case, and above
459 98% for the LDA case, are generally comparable and
460 competitive for most of the cases, they are also superior in
461 some of the comparisons. It is also interesting to note that
462 in our previous paper [12], the achieved results (86% after
463 PCA and 95% after LDA) are inferior to the ones presented
464 here. This can be attributed to the added entropy feature
465 and the feature normalization, applied before the analysis
466 and classification stages, but would need further investigation
467 in a future work.

469 References

- 470 1. Astel A, Tsakouski S, Barbieri S, Simeonov V (2007) Comparison of self-organizing maps classification approach with cluster
471 and principal components analysis for large environmental data
472 sets. *Water Res* 41:4566–4578
- 473 2. Chamundeeswari VV, Singh D, Singh K (2009) An analysis of
474 texture measures in PCA-based unsupervised classification of
475 SAR images. *IEEE Geosci Remote Sens Lett* 6:214–218
- 476 3. Ersoy O, Aydar E, Gourgaud A, Artuner H, Bayhan H (2007)
477 Clustering of volcanic ash arising from different fragmentation
478 mechanisms using Kohonen self-organizing maps. *Comput
479 Geosci* 33:821–828

- 481 4. Guler I, Demirhan A, Karakis R (2009) Interpretation of MR
482 images using self-organizing maps and knowledge-based expert
483 systems. *Digital Signal Process* 19:668–677
- 484 5. Lei Q, Zheng QF, Jiang SQ, Huang QG, Gao W (2008) Unsupervised
485 texture classification: automatically discover and classify texture
486 patterns. *Image Vis Comput* 26:647–656
- 487 6. Martens G, Poppe C, Lambert P, Van de Walle R (2008) Unsupervised
488 texture segmentation and labeling using biologically inspired
489 features. In: *IEEE 10th workshop on multimedia signal processing*, vols 1 and 2, pp 163–168
- 490 7. Paniagua B, Vega-Rodriguez MA, Gomez-Pulido JA, Sanchez-Perez
491 JM (2010) Improving the industrial classification of cork stoppers
492 by using image processing and neuro-fuzzy computing. *J Intell
493 Manuf* 21:745–760
- 494 8. Shih FY (2010) *Image processing and pattern recognition: fundamentals
495 and techniques*. Wiley, Hoboken
- 496 9. Umbaugh SE (2010) *Digital image processing and analysis*. CRC; Taylor & Francis, Boca Raton
- 497 10. Bishop CM (2004) *Neural networks for pattern recognition*. Clarendon Press, Oxford
- 498 11. Theodoridis S, Koutroubas K (2009) *Pattern recognition*. Elsevier/Academic Press, Amsterdam
- 499 12. Georgieva A, Jordanov I (2009) Intelligent visual recognition and classification of cork tiles with neural networks. *IEEE Trans Neural Netw* 20:675–685
- 500 13. Christodoulou CI, Pattichis CS, Pantziaris M, Nicolaides A (2003) Texture-based classification of atherosclerotic carotid plaques. *IEEE Trans Medical Imag* 22:902–912
- 501 14. Kuo CFJ, Kao CY (2007) Self-organizing map network for automatically recognizing color texture fabric nature. *Fibers Polym* 8:174–180
- 502 15. Salah M, Trinder J, Shaker A (2009) Evaluation of the self-organizing map classifier for building detection from lidar data and multispectral aerial images. *J Spatial Sci* 54:15–34
- 503 16. Liu H, Yu L (2005) Toward integrating feature selection algorithms for classification and clustering. *IEEE Trans Knowl Data Eng* 17:491–502
- 504 17. Haralick RM, Shanmuga K, Dinstein I (1973) Textural features for image classification. *IEEE Trans Syst Man Cybern Smc* 3: 610–621
- 505 18. Kohonen O, Hauta-Kasari M, Parkkinen J, Jaaskelainen T (2006) Co-occurrence matrix and self-organizing map based query from spectral image database. art. no. 603305, *ICO20: Illumination, Radiation, and Color Technologies*, vol 6033, pp 3305–3305
- 506 19. Randen T, Husoy JH (1999) Filtering for texture classification: a comparative study. *IEEE Trans Pattern Anal Mach Intell* 21: 291–310
- 507 20. Davies ER (2005) *Machine vision: theory, algorithms, practicalities*. Morgan Kaufmann, Amsterdam
- 508 21. Dillon WR, Goldstein M (1984) *Multivariate analysis: methods and applications*. Wiley, New York
- 509 22. Kohonen T (1990) The self-organizing map. *Proc IEEE* 78: 1464–1480
- 510
511
512
513
514
515
516
517
518
519
520
521
522
523
524
525
526
527
528
529
530
531
532
533
534